

# Magnetic Slow Relaxation in Cyclic Tb<sup>III</sup>-Nitronyl Nitroxide Radical Complexes

Haixia Tian,<sup>[a]</sup> Ruina Liu,<sup>[a]</sup> Xiaoling Wang,<sup>[a]</sup> Peipei Yang,<sup>[a]</sup> Zuoxi Li,<sup>[a]</sup> Licun Li,<sup>\*,[a]</sup> and Daizheng Liao<sup>[a]</sup>

**Keywords:** Radicals / Nitronyl nitroxide / Lanthanides / Terbium / Magnetic properties / Single molecule magnet

Two nitronyl nitroxide radical-Tb<sup>III</sup> complexes, [Tb(hfac)<sub>3</sub>-(NIT-3Py)]<sub>2</sub> (**1**) and [Tb(hfac)<sub>3</sub>(NIT-4Py)]<sub>2</sub> (**2**) {hfac = hexafluoroacetylacetonate; NIT-3Py = 2-(3'-pyridyl)-4,4,5,5-tetramethylimidazoline-1-oxyl 3-oxide; NIT-4Py = 2-(4'-pyridyl)-4,4,5,5-tetramethylimidazoline-1-oxyl 3-oxide} have been synthesized. Both complexes possess cyclic dimer structure in which each pyridyl-substituted radical links two different metal ions through the oxygen of nitroxide group and the

pyridine nitrogen. DC magnetic studies show the Tb<sup>III</sup> ion interacts ferromagnetically with the directly bonding nitronyl nitroxide. Complex **1** exhibits magnetic slow relaxation resembling SMM behavior, while there are no clearly the frequency-dependent out-of-phase signals for complex **2**.

(© Wiley-VCH Verlag GmbH & Co. KGaA, 69451 Weinheim, Germany, 2009)

## Introduction

The study of single-molecule magnets (SMMs) is currently one of the key topics in the field of molecular magnetism.<sup>[1–3]</sup> SMMs have been proposed as candidates for high-density information storage, in which each bit of information is stored as the magnetization orientation of an individual molecule, and quantum computation, in which the molecules can serve as qubits.<sup>[4–6]</sup> SMMs behavior is the result of the combination of a large ground state spin ( $S_T$ ) value and a significant uniaxial (Ising) magnetic anisotropy, as indicated by a negative value of the axial zero-field splitting (ZFS) parameter,  $D$ . Many different directions are being pursued in the study of SMMs.<sup>[7–9]</sup> One of them focuses on how to obtain the molecules with the large spin ground state ( $S_T$ ) so that increasing the energy barrier ( $\Delta$ ) that can be expressed as  $\Delta = |D|S_T^2$  (for integer spin) or  $\Delta = |D|(S_T^2 - 1/4)$  (for half-integer spin).<sup>[10]</sup> The exceptional efforts have lead to a significant increase in the spin ground state, with a record value as high as  $S = 83/2$ .<sup>[11]</sup> However, it has proved remarkably difficult to optimize both parameters and, the simply enhancing  $S_T$  is not as efficient as suggested by the previous rules for increasing the energy barrier ( $\Delta$ ).<sup>[12]</sup> Thus maximizing  $D$ , represents a new challenge.<sup>[13]</sup> As well known, lanthanide ions, especially heavy lanthanide ions such as terbium(III) and dysprosium(III), have a large anisotropy, utilization of the lanthanide ions has been one of the most elegant ways to design SMMs.<sup>[14,15]</sup> To date, a number of mixed lanthanide and transition metal ions<sup>[16]</sup> or radicals clusters<sup>[17]</sup> as well as

pure 4f metal systems<sup>[15b,18]</sup> have been reported. However, radical-lanthanide SMMs are relatively scarce. On the other hand, the lanthanide ions are often characterized by a fast tunneling of the magnetization and how to tune the quantum tunneling of the magnetization is another challenge in the SMMs.<sup>[12]</sup> Recently the studies show the introducing weak intermolecular antiferromagnetic interactions between the SMM units<sup>[19]</sup> and intramolecular weak magnetic coupling between the lanthanide ions<sup>[17]</sup> can tune the quantum properties. Hence it is worth exploring how to control the quantum tunneling of the lanthanide-based complexes. Here, we report two cyclic radical-Tb<sup>III</sup> complexes by using different pyridyl-substituted nitronyl nitroxide radicals, [Tb(hfac)<sub>3</sub>(NIT-3Py)]<sub>2</sub> (**1**) and [Tb(hfac)<sub>3</sub>-(NIT-4Py)]<sub>2</sub> (**2**) {hfac = hexafluoroacetylacetonate; NIT-3Py = 2-(3'-pyridyl)-4,4,5,5-tetramethylimidazoline-1-oxyl 3-oxide; NIT-4Py = 2-(4'-pyridyl)-4,4,5,5-tetramethylimidazoline-1-oxyl 3-oxide}, which exhibit different magnetic relaxation phenomenon.

## Results and Discussion

### Crystal Structure

Complex **1** crystallized in the monoclinic space group  $C2/c$ , while complex **2** crystallized in the monoclinic space group  $P2_1/n$ . The labeling Scheme for the crystal structures of complexes **1** and **2** are depicted in Figures 1 and 2, respectively. Selected bond parameters are listed in Tables 1 and 2. The molecular structures of complex **1** and **2** are similar. Both are central symmetric and two pyridine substituted radical ligands are coordinated to two Tb<sup>III</sup> ions through the oxygen atoms of the nitronyl nitroxide groups

[a] Department of Chemistry, Nankai University, Tianjin 300071, P. R. China  
E-mail: llicun@nankai.edu.cn

and the nitrogen atoms of the pyridine rings in *cis*-configuration to form a four-spin cyclic complex. The Tb<sup>III</sup> ion is octacoordinated and the Tb–N and Tb–O(nitroxide group) bond lengths are 2.601(4) and 2.319(4) Å for **1**, and 2.593(4) and 2.364(4) Å for **2**, which are comparable to those of the reported in other lanthanide–pyridine-substituted radical complexes.<sup>[17,20]</sup> The Tb–O–N angles are 136.4(3)° and 138.5(3)° for **1** and **2**, respectively. The bond angle formed by the coordinated oxygen atom of NO group and nitrogen atom of the pyridine ring with Tb is 104.34(13)° in complex **2**, which is larger than the corresponding the bond angle of 78.24(14)° in complex **1**. For the radical ligands, the dihedral angles between the O–N–C–N–O groups containing the unpair electron and the pyridine rings are 49.1 and 33.9° for **1** and **2**, respectively. In the dimer units, the distances of two metal ions are 6.957 Å for **1** and 7.879 Å for **2**. The shortest contacts between the uncoordinated NO groups in complex **1** and **2** are 4.922 and 8.707 Å, respectively, implying the complex molecules are well isolated.

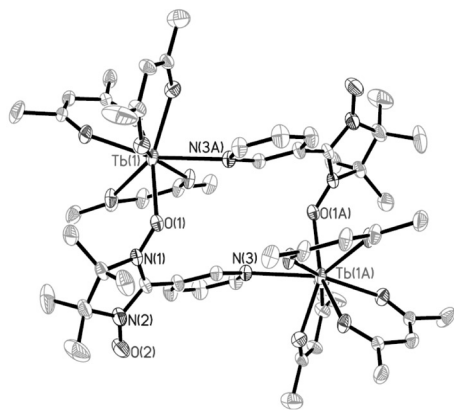


Figure 1. ORTEP drawing of complex **1** with the atom-labeling and 30% thermal ellipsoids. All hydrogen and fluorine atoms are omitted for clarity.

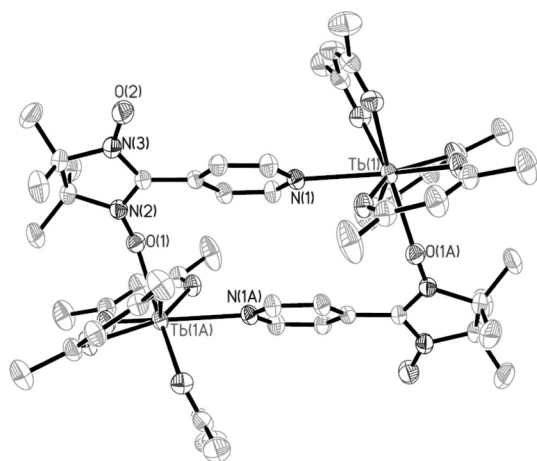


Figure 2. ORTEP drawing of complex **2** with the atom-labeling and 30% thermal ellipsoids. All hydrogen and fluorine atoms are omitted for clarity.

Table 1. Selected bond lengths [Å] and angles [°] for complex **1**.

Tb(1)–O(6)	2.313(4)	Tb(1)–O(7)	2.370(4)
Tb(1)–O(1)	2.319(4)	Tb(1)–O(4)	2.377(4)
Tb(1)–O(3)	2.336(3)	Tb(1)–N(3A)	2.601(4)
Tb(1)–O(8)	2.357(4)	O(1)–N(1)	1.297(6)
Tb(1)–O(5)	2.364(4)	O(2)–N(2)	1.273(7)
O(6)–Tb(1)–O(1)	107.21(14)	O(5)–Tb(1)–O(7)	129.69(15)
O(6)–Tb(1)–O(3)	135.84(13)	O(6)–Tb(1)–O(4)	73.58(15)
O(1)–Tb(1)–O(3)	89.81(14)	O(1)–Tb(1)–O(4)	74.70(14)
O(6)–Tb(1)–O(8)	85.89(15)	O(3)–Tb(1)–O(4)	72.26(14)
O(3)–Tb(1)–O(8)	107.78(15)	O(5)–Tb(1)–O(4)	76.39(16)
O(1)–Tb(1)–O(5)	149.51(15)	O(6)–Tb(1)–N(3A)	148.31(15)
O(3)–Tb(1)–O(5)	72.25(14)	O(1)–Tb(1)–N(3A)	78.24(14)
O(8)–Tb(1)–O(5)	71.26(15)	O(3)–Tb(1)–N(3A)	74.01(13)
O(6)–Tb(1)–O(7)	71.24(14)	O(8)–Tb(1)–N(3A)	71.89(15)
O(1)–Tb(1)–O(7)	75.98(14)	O(5)–Tb(1)–N(3A)	118.04(14)
O(3)–Tb(1)–O(7)	152.75(13)	O(7)–Tb(1)–N(3A)	80.32(13)
O(8)–Tb(1)–O(7)	71.81(14)	O(4)–Tb(1)–N(3A)	136.30(14)

Symmetry transformations used to generate equivalent atoms:

A:  $-x + 1/2, -y + 3/2, -z + 1$

Table 2. Selected bond lengths [Å] and angles [°] for complex **2**.

Tb(1)–O(7)	2.329(4)	Tb(1)–O(1A)	2.364(4)
Tb(1)–O(6)	2.344(4)	Tb(1)–O(3)	2.365(4)
Tb(1)–O(4)	2.345(4)	Tb(1)–N(1)	2.593(4)
Tb(1)–O(5)	2.350(4)	O(1)–N(2)	1.291(6)
Tb(1)–O(8)	2.361(4)	O(2)–N(3)	1.262(6)
O(7)–Tb(1)–O(6)	78.04(15)	O(8)–Tb(1)–O(1A)	145.50(14)
O(7)–Tb(1)–O(4)	105.04(15)	O(7)–Tb(1)–O(3)	141.84(14)
O(6)–Tb(1)–O(4)	144.98(13)	O(6)–Tb(1)–O(3)	126.27(13)
O(6)–Tb(1)–O(5)	73.15(13)	O(5)–Tb(1)–O(3)	134.40(14)
O(7)–Tb(1)–O(8)	71.08(14)	O(1A)–Tb(1)–O(3)	74.06(13)
O(6)–Tb(1)–O(8)	135.23(14)	O(7)–Tb(1)–N(1)	81.25(14)
O(4)–Tb(1)–O(8)	75.75(14)	O(6)–Tb(1)–N(1)	71.45(13)
O(5)–Tb(1)–O(8)	127.24(14)	O(4)–Tb(1)–N(1)	143.44(14)
O(7)–Tb(1)–O(1A)	143.32(14)	O(5)–Tb(1)–N(1)	141.33(14)
O(6)–Tb(1)–O(1A)	69.99(14)	O(8)–Tb(1)–N(1)	72.45(14)
O(4)–Tb(1)–O(1A)	91.81(14)	O(1A)–Tb(1)–N(1)	104.34(13)
O(5)–Tb(1)–O(1A)	77.25(13)	O(3)–Tb(1)–N(1)	80.61(13)

Symmetry transformations used to generate equivalent atoms:

A:  $-x + 1, -y + 2, -z + 1$

## Magnetic Properties

The temperature dependence of magnetic susceptibility of complex **1** and **2** was measured in 2–300 K range under the applied magnetic field of 2000 G and the magnetic behaviors are shown in Figure 3. At room temperature, the values of  $\chi_M T$  are 24.60 cm<sup>3</sup> K mol<sup>−1</sup> for **1** and 24.24 cm<sup>3</sup> K mol<sup>−1</sup> for **2**, close to expected value of 24.39 cm<sup>3</sup> K mol<sup>−1</sup> for two isolated Tb<sup>III</sup> (a <sup>7</sup>F<sub>6</sub> ion) and two uncorrelated  $S = 1/2$  spins. For complex **1**, the  $\chi_M T$  value almost is constant above 100 K, then gradually decreases to 24.32 cm<sup>3</sup> K mol<sup>−1</sup> at 40 K. Below 40 K, the  $\chi_M T$  value increases to a maximum of 25.27 cm<sup>3</sup> K mol<sup>−1</sup> at 9 K, then rapidly decreases to 22.23 cm<sup>3</sup> K mol<sup>−1</sup> at 2 K. For complex **2**, upon cooling, the  $\chi_M T$  value gradually decreases to reach a value of 22.43 cm<sup>3</sup> K mol<sup>−1</sup> at 14 K, below which  $\chi_M T$  rapidly increases to a maximum value of 23.18 cm<sup>3</sup> K mol<sup>−1</sup> at ca. 3.5 K, then decreases on further cooling. For both complexes, the decrease of  $\chi_M T$  on lowering of the tempera-

ture in the high temperature regime is most probably governed by the depopulation of the Tb Stark levels. The increase of  $\chi_M T$  at low temperature suggests the presence of intramolecular ferromagnetic interaction. For the present magnetic system, there are mainly three kinds of magnetic interactions, namely: (i) Tb<sup>III</sup> interacting with the directly coordinated NO group; (ii) Tb<sup>III</sup> interacting with the NO group through the pyridine ring; (iii) Tb<sup>III</sup>–Tb interaction via the radical ligand. The first magnetic coupling should be the strongest one. Therefore, the increase of  $\chi_M T$  at lower temperatures may be attributed to a ferromagnetic Tb-coordinated NO group interaction. The observed ferromagnetic interaction is agreement with those reported similar Ln<sup>III</sup>–radical complexes in the literature<sup>[17,20]</sup> and has been interpreted as the result of a spin polarization mechanism of the radicals' unpaired electrons on the Ln<sup>III</sup> empty orbitals. It is known that the coupled systems,<sup>[21]</sup> including at least one ion with an orbital momentum, are not amenable to a

quantitative analysis. The decrease of  $\chi_M T$  in the lowest temperature in complexes **1** and **2** may be ascribed to weak intramolecular Tb<sup>III</sup>–Tb, Tb–radical (via the pyridine ring) interactions, and/or intermolecular magnetic coupling.

To examine the spin dynamics, the temperature dependence of the ac magnetic susceptibility was collected at zero dc field with an ac field of 3 Oe with oscillating frequencies. Complex **1** shows frequency-dependent out-of-phase signals (Figure 4), which indicate the presence of slow magnetic relaxation of **1** at low temperature, but there is no maxima visible down to 2.0 K. As well know, the tunneling process can shorten the magnetic relaxation time at zero dc field, however, the tunneling mechanism can be suppressed by applying a static magnetic field.<sup>[22]</sup> So we recorded ac susceptibility vs. temperature in 3 kOe dc field. As a result, both in-phase and out-of-phase frequency-dependent signals are more visible and appear the maxima. The peak temperatures of  $\chi''$  can be fitted by Arrhenius law (Figure 5),  $\tau = \tau_0 \exp(\Delta/k_B T)$ , which gives the pre-exponential factor  $\tau_0 = 8.8(3) \times 10^{-8}$  s and the effective anisotropy barrier  $\Delta/k_B = 19.0(6)$  K, in accordance with the behaviour of SMMs.<sup>[23]</sup> The obtained values of  $\tau_0$  and  $\Delta$  are comparable to those of reported Tb-based SMMs.<sup>[14a,14e,24]</sup> For complex **2**, no clearly frequency-dependent out-of-phase signals were observed above 2 K as shown in Figure 6, due to fast tunneling relaxation process. As seen, although two complexes show the similar crystal structure, they exhibit different magnetic slow relaxation. One hand, in fact, there are the slightly different morphology of the ligand field for complex **1** and **2**, mainly originating from the different O–Tb–N angles. On the other hand, the magnetic interactions mediated by two radical ligands are different. NIT-3Py ligand should produce stronger magnetic exchange coupling due to its pyridyl nitrogen atom with the higher spin density, which results in the stronger magnetic interaction between

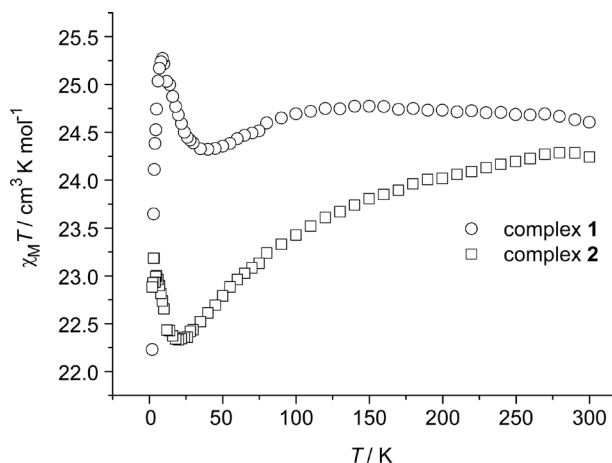


Figure 3. Plots of  $\chi_M T$  vs.  $T$  for complex **1** and **2**.

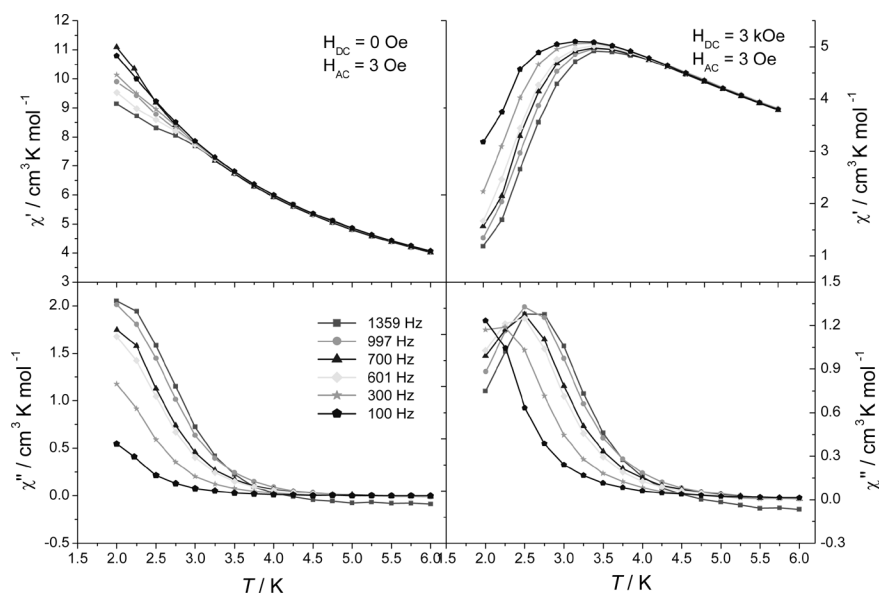


Figure 4. Temperature dependence of the in-phase (top) and out-of-phase (bottom) components of ac susceptibility for **1** in zero (left) and a 3 kOe (right) dc field with an oscillation of 3 Oe.

two Tb<sup>III</sup> ions in **1**. Thus the origin of different magnetic relaxation in **1** and **2** may be from the different ligand field effect and/or the different magnetic coupling between Tb<sup>III</sup> ions.

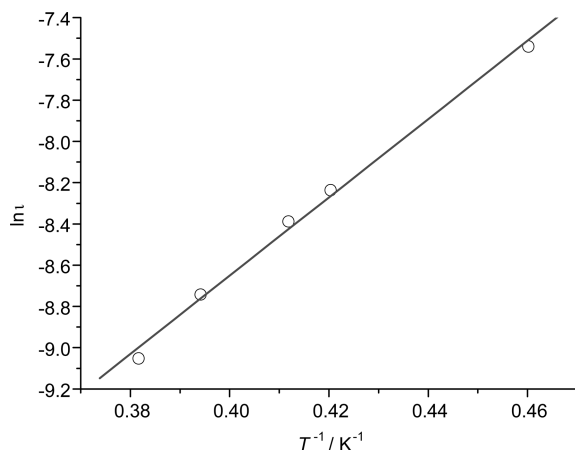


Figure 5. Arrhenius plot for **1** in a 3 kOe static field. Solid line represents the best linear fit of the data.

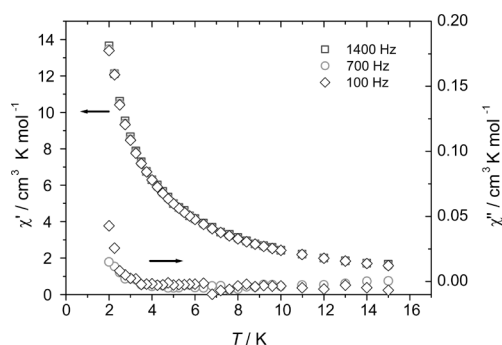


Figure 6. Temperature dependence of the in-phase and out-of-phase components of ac susceptibility for **2** in zero dc field with an oscillation of 3 Oe.

## Conclusions

We use non-chelating pyridine substituted nitronyl nitroxide radical ligands to obtain two radical-lanthanide complexes with similar crystal structure, but they show different magnetic relaxation phenomenon. Our works show that the slightly different ligand field and magnetic exchange coupling between metal ions can drastically affects the tunneling of the magnetization.

## Experimental Section

**Materials:** All the starting chemicals were of AR grade and used as received. The radical ligands NIT-3Py and NIT-4Py were prepared according to literature methods.<sup>[25]</sup>

**Physical Measurements:** Elemental analyses (C, H, N) were carried out with a Perkin–Elmer 240 elemental analyzer. The infrared spectra were recorded from KBr pellets in the range 4000–400 cm<sup>−1</sup> with a Bruker Tensor 27 IR spectrometer. The magnetic measure-

ments were performed with an MPMS XL-7 SQUID magnetometer. Diamagnetic corrections were made with Pascal's constants for all the constituent atoms.

**[Tb(hfac)<sub>3</sub>(NIT-3Py)<sub>2</sub>] (1):** 32 mg(0.04 mmol) of Tb(hfac)<sub>3</sub>·2H<sub>2</sub>O was dissolved in 30 mL of boiling heptane to azeotropically remove hydration water molecules. After that, the solution was cooled to 80 °C, and a solution of NIT-3Py (9.8 mg, 0.04 mmol) in 2 mL of CH<sub>2</sub>Cl<sub>2</sub> was added. The resulting solution was stirred for 5 min and then cooled it to room temperature. The filtrate was allowed to stand at room temperature for slow evaporation. After one week, the purple crystals were collected; yield 60%. C<sub>54</sub>H<sub>38</sub>F<sub>36</sub>N<sub>6</sub>O<sub>16</sub>Tb<sub>2</sub> (2028.74): calcd. C 31.97, H 1.89, N 4.14; found C 31.70, H 1.58, N 4.20. FT-IR (KBr):  $\tilde{\nu}$  = 1651 (s), 1617 (m), 1559 (m), 1500 (s), 1257 (s), 1207 (s), 1147 (s), 802 (m), 661 (m) cm<sup>−1</sup>.

**[Tb(hfac)<sub>3</sub>(NIT-4Py)<sub>2</sub>] (2):** Complex **2** was synthesized using the same procedure for complex **1** but with NIT-4Py instead of NIT-3Py. C<sub>54</sub>H<sub>38</sub>F<sub>36</sub>N<sub>6</sub>O<sub>16</sub>Tb<sub>2</sub> (2028.74): calcd. C 31.97, H 1.89, N 4.14; found C 31.51, H 2.01, N 4.51; yield 68%. FT-IR (KBr):  $\tilde{\nu}$  = 1672 (s), 1566 (s), 1258 (s), 1203 (s), 1170 (s), 1149 (s), 792 (m), 654 (m) cm<sup>−1</sup>.

**X-Ray Crystallography:** Diffraction intensity data were collected on a Rigaku Saturn CCD diffractometer for **1** at 113 K and Rigaku SCXmini diffractometer for **2** at room temperature employing graphite-monochromated Mo-K $\alpha$  radiation ( $\lambda$  = 0.71073 Å). The structure was solved by direct methods by using the program SHELXS-97<sup>[26]</sup> and refined by full-matrix least-squares methods on  $F^2$  with the use of the SHELXL-97<sup>[27]</sup> program package. Anisotropic thermal parameters were assigned to all non-hydrogen atoms. The hydrogen atoms were set in calculated positions and refined as riding atoms with a common fixed isotropic thermal parameter. Disordered carbon atoms were observed in the hfac ligands for complex **1** and disorders were also observed for some fluorine atoms. The pertinent crystallographic data and structure refinement parameters for complexes **1** and **2** were listed in Table 3.

Table 3. Crystal data and structure refinement for **1** and **2**.

	<b>1</b>	<b>2</b>
Empirical formula	C <sub>54</sub> H <sub>38</sub> F <sub>36</sub> N <sub>6</sub> O <sub>16</sub> Tb <sub>2</sub>	C <sub>54</sub> H <sub>38</sub> F <sub>36</sub> N <sub>6</sub> O <sub>16</sub> Tb <sub>2</sub>
$M_r$	2028.74	2028.74
$T$ / K	113(2)	293(2)
$\lambda$ (Mo-K $\alpha$ ) / Å	0.71073	0.71073
Crystal system	monoclinic	monoclinic
Space group	$C2/c$	$P2_1/n$
$a$ / Å	30.492(6)	17.138(3)
$b$ / Å	11.554(2)	12.198(2)
$c$ / Å	20.464(4)	18.423(4)
$\beta$ / deg	93.99(3)	92.75(3)
$V$ / Å <sup>3</sup>	7192(2)	3846.9(13)
$Z$	4	2
$D_c$ / g cm <sup>−3</sup>	1.874	1.751
$\mu$ / mm <sup>−1</sup>	2.110	1.972
$\theta$ range / deg	1.89–25.02	3.06–25.02
Unique reflections, $R_{int}$	6339, 0.0402	6775, 0.0456
GOF	1.095	1.116
$R1^{[a]}$ [ $I > 2\sigma(I)$ ]	0.0460	0.0483
$wR2^{[b]}$ (all data)	0.1206	0.1080

[a]  $R1 = \sum(|F_o| - |F_c|) / \sum|F_o|$ . [b]  $wR2 = \{\sum w(|F_o|^2 - |F_c|^2)^2 / \sum w|F_o|^2\}^{1/2}$ .

CCDC-737320 (for **1**) and -737321 (for **2**) contain the supplementary crystallographic data for this paper. These data can be obtained free of charge from The Cambridge Crystallographic Data Centre via [www.ccdc.cam.ac.uk/data\\_request/cif](http://www.ccdc.cam.ac.uk/data_request/cif).



## Acknowledgments

This work was supported by the National Natural Science Foundation of China (50672037, 20471032) and the Natural Science Foundation of Tianjin (09JCYBJC05600).

- [1] a) D. Gatteschi, R. Sessoli, *Angew. Chem. Int. Ed.* **2003**, *42*, 268–297; b) R. Sessoli, D. Gatteschi, A. Caneschi, M. A. Novak, *Nature* **1993**, *365*, 141–143; c) D. Gatteschi, R. Sessoli, J. Villain, *Molecular Nanomagnets*, Oxford University Press, Oxford, **2006**.
- [2] a) R. Sessoli, H. L. Tsai, A. R. Schake, S. Wang, J. B. Vincent, K. Folting, D. Gatteschi, G. Christou, D. N. Hendrickson, *J. Am. Chem. Soc.* **1993**, *115*, 1804–1806; b) M. Murugesu, W. Wernsdorfer, K. A. Abboud, G. Chistou, *Angew. Chem. Int. Ed.* **2005**, *44*, 892–896.
- [3] a) R. Bircher, G. Chaboussant, C. Dobe, H. U. Güdel, S. T. Ochsenbein, A. Sieber, O. Waldmann, *Adv. Funct. Mater.* **2006**, *16*, 209–220; b) S. M. J. Aubin, N. R. Dilley, L. Pardi, J. Krzystek, M. W. Wemple, L.-C. Brunel, M. B. Maple, G. Christou, D. N. Hendrickson, *J. Am. Chem. Soc.* **1998**, *120*, 4991–5004; c) H. Oshio, M. Nakano, *Chem. Eur. J.* **2005**, *11*, 5178–5185.
- [4] D. Gatteschi, R. Sessoli, A. Cornia, *Chem. Commun.* **2000**, 725–732.
- [5] a) M. N. Leuenberger, D. Loss, *Nature* **2001**, *410*, 789–793; b) S. Hill, R. S. Edwards, N. Aliaga-Alcalde, G. Christou, *Science* **2003**, *302*, 1015–1018.
- [6] F. Meier, J. Levy, D. Loss, *Phys. Rev. Lett.* **2003**, *90*, 047901.
- [7] D. Ruiz-Molina, M. Mas-Torrent, J. Gómez, A. I. Balana, N. Domingo, J. Tejada, M. T. Martinez, C. Rovira, J. Veciana, *Adv. Mater.* **2003**, *15*, 42–45.
- [8] A. Cornia, A. C. Fabretti, M. Pacchioni, L. Zoppi, D. Bonacchi, A. Caneschi, D. Gatteschi, R. Biagi, U. Del Pennino, V. De Renzi, L. Gurevich, H. S. J. Van der Zant, *Angew. Chem. Int. Ed.* **2003**, *42*, 1645–1648.
- [9] M. Clemente-León, H. Soyer, E. Coronado, C. Mingotaud, C. J. Gómez-García, P. Delhaès, *Angew. Chem. Int. Ed.* **1998**, *37*, 2842–2845.
- [10] E.-C. Yang, W. Wernsdorfer, L. N. Zakharov, Y. Karaki, A. Yamaguchi, R. M. Isidro, G.-D. Lu, S. A. Wilson, A. L. Rheingold, H. Ishimoto, D. N. Hendrickson, *Inorg. Chem.* **2006**, *45*, 529–546.
- [11] A. M. Ako, I. J. Hewitt, V. Mereacre, R. Clérac, W. Wernsdorfer, C. E. Anson, A. K. Powell, *Angew. Chem. Int. Ed.* **2006**, *45*, 4926–4929.
- [12] R. Sessoli, *Inorg. Chim. Acta* **2008**, *361*, 3356–3364.
- [13] a) O. Waldmann, *Inorg. Chem.* **2007**, *46*, 10035–10037; b) E. Ruiz, J. Cirera, J. Cano, S. Alvarez, C. Loose, J. Kortus, *Chem. Commun.* **2008**, 52–54.
- [14] a) S. Osa, T. Kido, N. Matsumoto, N. Re, A. Pochaba, J. Mrozinski, *J. Am. Chem. Soc.* **2004**, *126*, 420–421; b) C. M. Zaleski, E. C. Depperman, J. W. Kampf, M. L. Kirk, V. L. Pecoraro, *Angew. Chem. Int. Ed.* **2004**, *43*, 3912–3914; c) A. Mishra, W. Wernsdorfer, K. A. Abboud, G. Christou, *J. Am. Chem. Soc.* **2004**, *126*, 15648–15649; d) C. Aronica, G. Pilet, G. Chastanet, W. Wernsdorfer, J.-F. Jacquot, D. Luneau, *Angew. Chem. Int. Ed.* **2006**, *45*, 4659–4662; e) J.-P. Costes, F. Dahan, W. Wernsdorfer, *Inorg. Chem.* **2006**, *45*, 5–7.
- [15] a) N. Ishikawa, M. Sugita, T. Ishikawa, S. Koshihara, Y. Kaizu, *J. Am. Chem. Soc.* **2003**, *125*, 8694–8695; b) J.-K. Tang, I. Hewitt, N. T. Madhu, G. Chastanet, W. Wernsdorfer, C. E. Anson, C. Benelli, R. Sessoli, A. K. Powell, *Angew. Chem. Int. Ed.* **2006**, *45*, 1729–1733.
- [16] a) E. J. Schelter, A. V. Prosvirin, K. R. Dunbar, *J. Am. Chem. Soc.* **2004**, *126*, 15004–15005; b) V. Mereacre, A. M. Ako, R. Clérac, W. Wernsdorfer, G. Filoti, J. Bartolomé, C. E. Anson, A. K. Powell, *J. Am. Chem. Soc.* **2007**, *129*, 9248–9249; c) F. Pointillart, K. Bernot, R. Sessoli, D. Gatteschi, *Chem. Eur. J.* **2007**, *13*, 1602–1609.
- [17] G. Poneti, K. Bernot, L. Bogani, A. Caneschi, R. Sessoli, W. Wernsdorfer, D. Gatteschi, *Chem. Commun.* **2007**, 1807–1809.
- [18] a) M. T. Gamer, Y. Lan, P. W. Roesky, A. K. Powell, R. Clérac, *Inorg. Chem.* **2008**, *47*, 6581–6583; b) Y.-Z. Zheng, Y. Lan, C. E. Anson, A. K. Powell, *Inorg. Chem.* **2008**, *47*, 10813–10815.
- [19] W. Wernsdorfer, N. Aliaga-Alcalde, D. N. Hendrickson, G. Christou, *Nature* **2002**, *416*, 406–409.
- [20] a) C. Benelli, A. Caneschi, D. Gatteschi, L. Pardi, *Inorg. Chem.* **1992**, *31*, 741–746; b) J.-X. Xu, Y. Ma, G.-F. Xu, C. Wang, D.-Z. Liao, Z.-H. Jiang, S.-P. Yan, L.-C. Li, *Inorg. Chem. Commun.* **2008**, *11*, 1356–1358.
- [21] a) M. L. Kahn, C. Mathonière, O. Kahn, *Inorg. Chem.* **1999**, *38*, 3692–3697; b) J. P. Costes, F. Dahan, A. Dupuis, J. P. Laurent, *Chem. Eur. J.* **1998**, *4*, 1616–1620.
- [22] L. Thomas, F. Lionti, R. Ballou, D. Gatteschi, R. Sessoli, B. Barbara, *Nature* **1996**, *383*, 145–147.
- [23] a) C. Sangregorio, T. Ohm, C. Paulsen, R. Sessoli, D. Gatteschi, *Phys. Rev. Lett.* **1997**, *78*, 4645–4648; b) V. Mereacre, A. M. Ako, R. Clérac, W. Wernsdorfer, I. J. Hewitt, C. E. Anson, A. K. Powell, *Chem. Eur. J.* **2008**, *14*, 3577–3584.
- [24] J. P. Costes, S. Shova, W. Wernsdorfer, *Dalton Trans.* **2008**, 1843–1849.
- [25] M. S. Davis, K. Morokuma, R. W. Kreilick, *J. Am. Chem. Soc.* **1972**, *94*, 5588–5592.
- [26] G. M. Sheldrick, *SHELXS-97: Program for the Solution of Crystal Structures*, University of Göttingen, Germany, **1997**.
- [27] G. M. Sheldrick, *SHELXL-97: Program for the refinement of Crystal Structures*, University of Göttingen, Germany, **1997**.

Received: June 25, 2009

Published Online: September 2, 2009